



Rifted continental margins: The case for depth-dependent extension

Ritske S. Huismans ^{a,*}, Christopher Beaumont ^b

^a Department of Earth Science, Bergen University, Bergen N-5007, Norway

^b Department of Oceanography, Dalhousie University, Halifax NS B3H 4J1, Canada

ARTICLE INFO

Article history:

Received 25 June 2014

Received in revised form 17 September 2014

Accepted 19 September 2014

Available online 13 October 2014

Editor: P. Shearer

Keywords:

rifted passive margins

geodynamics

basin evolution

forward modelling

ABSTRACT

Even though many basic properties of non-volcanic rifted margins are predicted by uniform extension of the lithosphere, uniform extension fails to explain other important characteristics. Particularly significant discrepancies are observed at: 1) the Iberia–Newfoundland conjugate margins (Type I), where large tracts of continental mantle lithosphere are exposed at the seafloor, and at 2) ultra-wide central South Atlantic margins (Type II) where continental crust spans wide regions below which it appears that lower crust and mantle lithosphere were removed. Neither corresponds to uniform extension in which crust and mantle thin by the same factor. Instead, either the crust or mantle lithosphere has been preferentially removed during extension. We show that the Type I and II styles are respectively reproduced by dynamical numerical lithospheric stretching models (Models I-A/C and II-A/C) that undergo depth-dependent extension. In this notation A and C imply underplating of the rift zone during rifting by asthenosphere and lower cratonic lithosphere, respectively. We also present results for models with a weak upper crust and strong lower crust, Models III-A/C, to show that lower crust can also be removed from beneath the rift zone by horizontal advection with the mantle lithosphere. From the model results we infer that these Type I, II, and III margin styles are controlled by the strength of the mid/lower crust, which determines the amount of decoupling between upper and lower lithosphere during extension and the excision of crust or mantle. We also predict the styles of sedimentary basins that form on these margins as a test of the concepts presented.

© 2014 Elsevier B.V. All rights reserved.

1. Introduction

Thirty-five years ago Dan McKenzie (1978) introduced the now widely accepted lithospheric stretching model for the formation and evolution of extensional basins and rifted continental margins. His uniform extension (UE) (pure shear) kinematic model explains many of their basic properties. However, as observations have improved in recent years it now appears that uniform extension fails to explain other important characteristics, leading to the present situation where we strongly suspect UE is too simple (Fraser et al., 2007). McKenzie's model assumes that the lithosphere undergoes UE, i.e. extension that is uniform with depth but varies laterally. It, like the corresponding derivative models, including depth-dependent extension (Royden and Keen, 1980; Kusznir and Karner, 2007), simple shear (Wernicke, 1981, 1985), detachment (Lister et al., 1986, 1991) and other compound models (Wernicke, 2009; Huismans and Beaumont, 2002, 2003) do not provide insight into the mechanics because they are kinematic descriptions. We don't even know when UE is favored. From a

mechanical viewpoint this leaves us with the knowledge that UE is a quite good first approximation, and that other modes can be expected, e.g. Buck's (1991) analysis and general classification of narrow, wide and core complex rift modes. However, we have no overarching quantitative general model for styles of lithospheric extension, as is evidenced by the recent review by Cloetingh et al. (2013), particularly when the lithosphere acts as a laminate with horizontal decoupling and shear among the layers. Analytical and numerical models that address this decoupled system do, however, suggest it leads to depth-dependent extension (e.g. Zuber et al., 1986; Huismans and Beaumont, 2003, 2008; Nagel and Buck, 2007; Weinberg et al., 2007; Kusznir and Karner, 2007).

Despite the lack of an overarching general understanding we can identify end-member situations that deviate from UE the most. Particularly significant discrepancies are observed at: 1) the Iberia–Newfoundland conjugate margins (which we call Type I), where the continental crust thins across a narrow region and large tracts of continental mantle lithosphere are exposed at the seafloor (Dean et al., 2000; Whitmarsh et al., 2001; Funck et al., 2003; Péron-Pinvidic et al., 2013; Sibuet and Tucholke, 2013), and at 2) ultra-wide central South Atlantic margins (which we call Type II) where thin, 'hyperextended', continental crust spans

* Corresponding author.

E-mail address: ritske.huismans@geo.uib.no (R.S. Huismans).

wide regions below which it appears that continental mantle lithosphere was removed (Meyers et al., 1996; Rosendahl et al., 2005; Contrucci et al., 2004; Moulin et al., 2005; Huismans and Beaumont, 2008; Aslanian et al., 2009; Sibuet and Tucholke, 2013). Neither of these styles corresponds to uniform extension in which crust and mantle thin equally. Instead, either the crust or mantle lithosphere has been preferentially removed.

In this paper we amplify our previous research that uses numerical models of continental lithospheric stretching to investigate the properties that lead to Type I and Type II styles of extension, and by inference, their natural equivalents. This approach was used by Huismans and Beaumont (2008) and the Type I and Type II styles were explicitly introduced in Huismans and Beaumont (2011). We also demonstrate an additional depth-dependent mechanism, lower lithosphere counterflow, to explain exposure of large regions of continental mantle lithosphere in the outer region of a margin, as noted above. In this concept buoyant lower continental lithosphere flows laterally and underplates the rift axis ahead of the upwelling asthenosphere as was demonstrated by Huismans and Beaumont (2011) and Beaumont and Ings (2012).

We present the case that the contrasting characteristics described above are a consequence of depth-dependent lithospheric extension (Kusznir and Karner, 2007), and that the Type I and Type II margin styles represent end members (Contrucci et al., 2004; Moulin et al., 2005; Huismans and Beaumont, 2008; Aslanian et al., 2009; Sibuet and Tucholke, 2013; Pérön-Pinvidic and Manatschal, 2009; Pérön-Pinvidic et al., 2013). We build on the brief, partial set of results (Huismans and Beaumont, 2011) and use a complete set of consistent models to illustrate our hypothesis that these styles are a direct consequence of the properties of the mid/lower crust, which determines the amount and level of decoupling, and style of excision between upper and lower lithosphere during extension. We first list the characteristics of Type I and Type II margins. Models I demonstrate that strong coupling between rheological layers reproduces the Type I style of the Iberia–Newfoundland system. Models II, which have weak crustal layers that allow decoupling during extension, reproduce characteristics of Type II margins. Models III, which we introduce here, have a weak mid-crust but strong lower crust. They also decouple, but within the mid-crust, and demonstrate a contrasting mechanism for removing lower crust from beneath the rift. We lack a clear example of the corresponding natural Type III margin.

For each of the Model I–III types we also consider the role of asthenospheric upwelling beneath the rift axis (A models) versus cratonic underplating by lower lithosphere counterflow (C models). Lastly, we describe the characteristics of sedimentary basins that form on Model I–III margins and propose these as templates to be used as direct tests of the concepts presented.

2. Characteristics of the Type I and Type II rifted margins

The defining characteristics of Type I non-volcanic margins (e.g., Iberia–Newfoundland, Pérön-Pinvidic and Manatschal, 2009; Van Avendonk et al., 2009; Sibuet and Tucholke, 2013; Sutra et al., 2013) and Labrador–Southern Greenland (Keen et al., 1994, 2012; Chian et al., 1995; Louden and Chian, 1999) conjugate margins (Fig. 1a) are listed below in order of their development. Following distributed deformation (Huismans and Beaumont, 2007), which may lead to the formation of offset rift basins (Beaumont and Ings, 2012; Chenin and Beaumont, 2013), extension becomes focused in one region and is characterized as follows (Fig. 1a, 1–7): 1) development of major basin forming faults/shears that penetrate into the crust possibly rooting in the lower crust; 2) formation of narrow transitional regions (<100 km wide) where the continental crust thins abruptly; 3) a clearly asymmetric geometry in some cases and uplift of rift flanks; 4) breakup of the crust before

breakup of the mantle lithosphere; 5) exhumation and exposure, or near exposure, of serpentinized continental mantle lithosphere in the transition between continental and oceanic crust (OCT); 6) relatively little surface magmatism during rifting; 7) oceanic crust that is initially thin, and late stage establishment of a magmatic ocean spreading centre. Examples from the Newfoundland–Iberia conjugate margins (Figs. 1b–d) illustrate these Type I characteristics. The focus is on the central rift and not the offset rift basins. Some of these characteristics are still debated (see Sibuet and Tucholke, 2013 for a recent review). For example, Jagoutz et al. (2007) present the case for magma-starved embryonic oceanic crust which would be thin, and Van Avendonk et al. (2006) and Hopper et al. (2007) interpret seismic data to support this thin oceanic crust. However, in a recent reanalysis Minshull et al. (2014) interpret it to be normal thickness.

In contrast, Type II margins (e.g. some wide margins in the central South Atlantic (Contrucci et al., 2004; Moulin et al., 2005; Huismans and Beaumont, 2008; Aslanian et al., 2009; Sibuet and Tucholke, 2013; Pérön-Pinvidic et al., 2013; Kumar et al., 2013), and the Exmouth plateau (Kusznir and Karner, 2007) (Fig. 1e, A–I), are characterized by: A) ultra-wide (>350 km) regions of very thin continental crust, with little evidence for a lower crustal layer; B) faulted early syn-rift sedimentary basins; C) undeformed late syn-rift sediments (but also including salt deformed by gravitational flow in some instances); D) sediments deposited under demonstrated shallow marine or lacustrine-fluvial conditions in syn-rift ‘sag’ basins, leading to the inference; E) that continental mantle lithosphere has been replaced by hot asthenosphere beneath large regions of the margin; F) lack of mechanical flexural flank uplifts of the crust; G) no clear evidence of exposed exhumed mantle lithosphere; H) limited magmatism during rifting, with lower crustal seismic layers with velocities consistent with magmatic underplating, and seaward dipping reflectors in some cases, and; I) a mature magmatic mid-oceanic ridge established system soon after crustal breakup and normal thickness oceanic crust. These properties are illustrated (Fig. 1f) for two South Atlantic margins. Some of the characteristics are also observed in the Basin and Range (Fig. 1g) (Jones et al., 1992, Fig. 6; Wernicke, 2009), which we consider as an early stage underdeveloped analogue of rifted margins where lower crust has yet to be removed. To be clear, some Type II African and South American margins are elevated but this is interpreted to result from regional mantle induced dynamical uplift, magmatic underplating, or other mechanisms, for example compression (e.g. Japsen et al., 2012), that do not have the short wavelength lithospheric flexural characteristics observed at Type I margins.

A particular characteristic of Type II margins is the absence of seismically identified lower crust beneath much of the margin (Figs. 1e, f) (Karner et al., 2003; Sibuet and Tucholke, 2013), or that it is highly attenuated. An example is the Angola margin where the Moulin et al. (2005) crustal velocity model shows only extremely thin (~1 km thick) regions where the seismic velocity exceeds 6.7 km/s, which would commonly be interpreted as characteristic of lower crust. Assuming lower crust was present before rifting started, there is a need to understand what has happened to this layer. Aslanian and Moulin (2013) have followed Karner et al. (1997, 2003) in drawing attention to this problem, specifically in the context of ‘balancing’ the crustal cross sectional area of the margins. It appears that the final upper crust contains added ‘allochthonous crust’, which was not part of the original mid/upper crust. One mechanism that removes lower crust and creates ‘allochthonous crust’ is formation of metamorphic core complexes, as in the Basin and Range (Fig. 1g). We suggest below that structures analogous to those in the Basin and Range may be present in Type II margins. In addition, ductile lower continental crust may flow to the distal regions of the margin during rifting

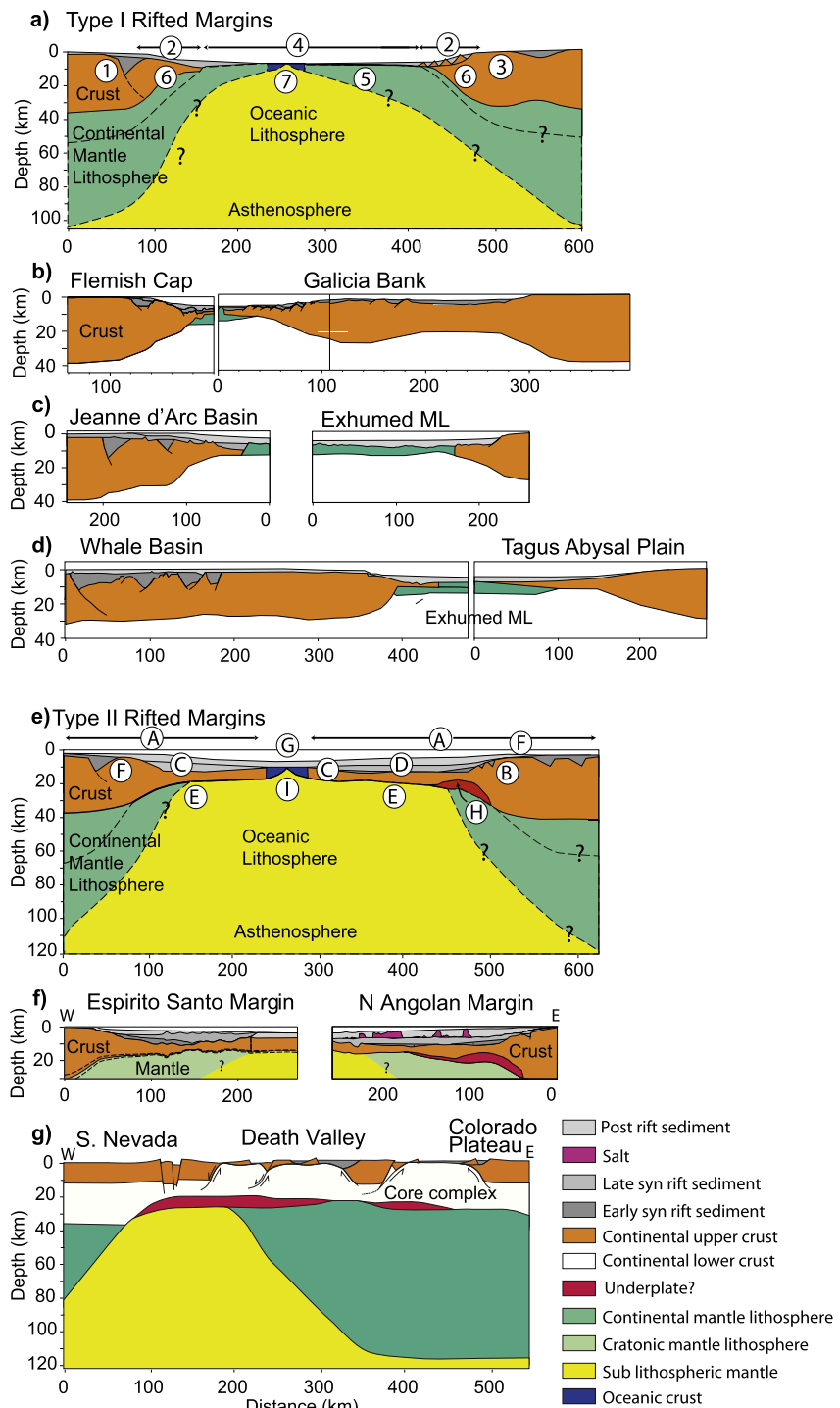


Fig. 1. Diagram showing characteristic properties of: a) Type I and e) Type II rifted continental margins based on observations from the Iberia–Newfoundland conjugate margins and central South Atlantic margins, respectively (Dean et al., 2000; Whitmarsh et al., 2001; Funck et al., 2003; Meyers et al., 1996; Rosendahl et al., 2005; Conracci et al., 2004; Moulin et al., 2005). See text for characteristics 1–7 and A–I. b)–d) Northern, central and southern crustal conjugate cross sections for the Iberia–Newfoundland margin system based on seismic reflection data, and gravity inversion (Funck et al., 2003; Pérez-Gussinyé et al., 2003). Note older offset rift basins, short crustal thinning length scale adjacent to oceanic crust, thin crustal wedge on top of mantle lithosphere, and exhumed mantle lithosphere in ocean–continent-transition zone. f) Interpreted conjugate cross section of central South Atlantic margins. Note highly stretched crustal cross section, possibly underlain by depleted cratonic mantle lithosphere, and late syn-rift salt deposits (magenta) (Conracci et al., 2004; Rosendahl et al., 2005). g) Cross section through the Basin and Range extensional province (modified after Jones et al., 1992). Note distributed crustal extension, core complex formation, flat Moho topography and inferred mid/lower crustal flow, and narrow localized necking of the mantle lithosphere.

(Huismans and Beaumont, 2008, 2011; Sibuet and Tucholke, 2013). This happens today at D’Entrecasteaux Island in the Woodlark Basin (Little et al., 2007, 2011). The islands forming at the propagating rift axis are gneiss domes/metamorphic core complexes, comprising laterally flowing, likely diapirically rising lower crust.

Model II-A (Figs. 4a, b) is very similar to a cartoon representing the lithospheric-scale structure below the islands (Eilon et al., 2014, Fig. 12) and brackets the estimated extension, 140–190 km. It shows the same dramatic thinning/removal of the mantle lithosphere. The style of lateral flow and emplacement of the gneiss

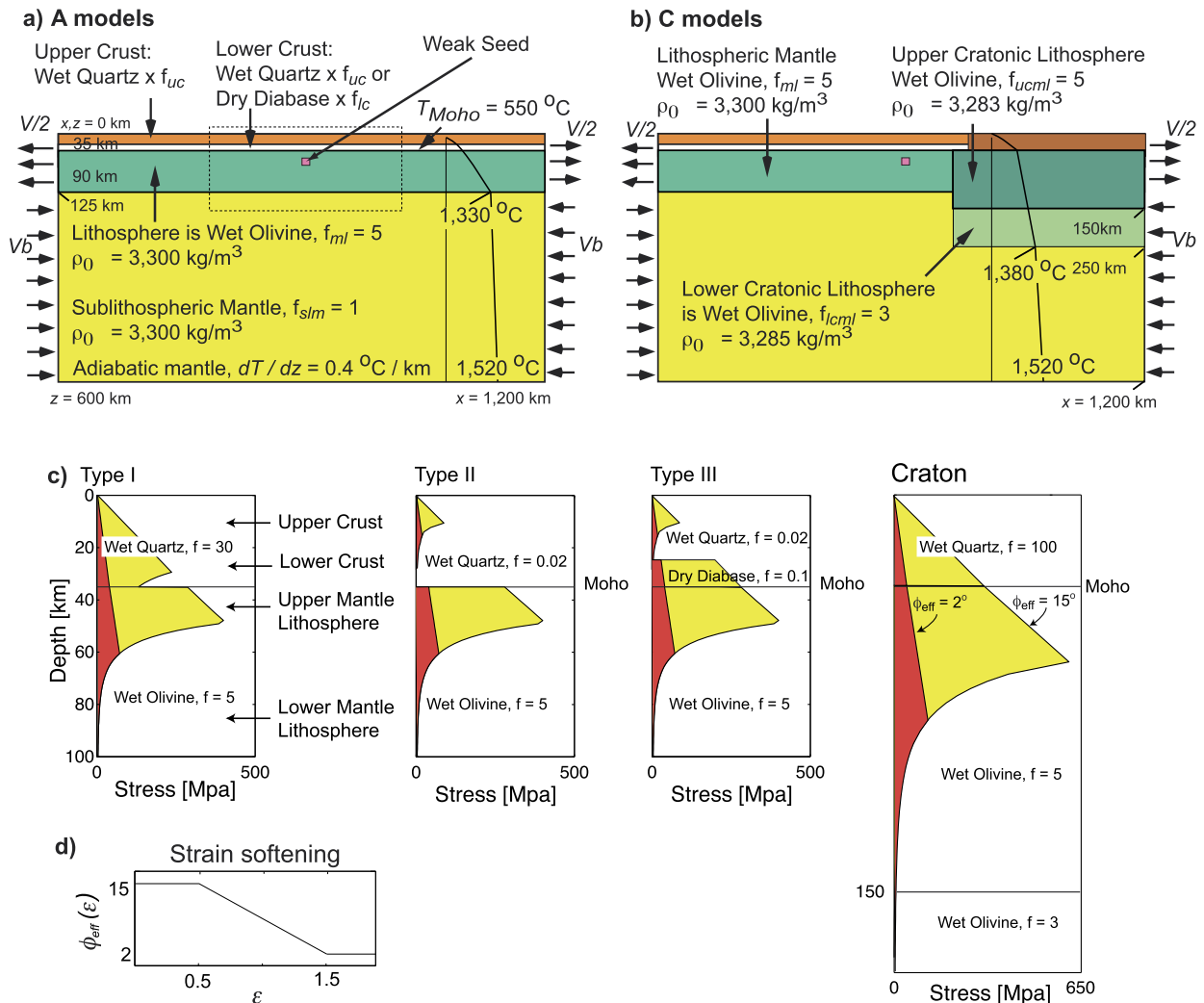


Fig. 2. Numerical model design. a) A models have standard lithosphere that is 125 km thick, crustal thickness 35 km, and are laterally uniform except for a small weak seed used to localize deformation. b) C models have a 250 km thick embedded cratonic region to the right of the weak seed but the crust remains 35 km thick. We do not appeal to rifting of cratonic lithosphere in C models but, instead, consider rifts that develop close to a craton boundary which is more common. In this case lower lithosphere counterflow is asymmetric. Horizontal velocity boundary conditions of $\pm V/2$ (where $V = 1.5 \text{ cm a}^{-1}$) are applied to the lithosphere and the corresponding exit flux is balanced by a low velocity inflow in the sublithospheric mantle, V_b . The top is a free surface. The sides are free slip, and the base is a horizontal free slip boundary. Materials deform viscously except when the material is at plastic yield. c) Rheological stratification for Models Types I-A, II-A, III-A and Cratonic lithosphere for a nominal strain rate of 10^{-14} s^{-1} . Materials listed give the laboratory flow laws for the reference materials and are modified by the scaling factor f as explained in the Methods Appendix A. Crustal flow is based on wet quartzite (WQz, Gleason and Tullis, 1995) with scaling factors $f = 30$ (Type I), $f = 0.02$ (Types II and III), and $f = 100$ (Craton). Strong lower crust (Type III) is based on dry Maryland diabase (DMD, Mackwell et al., 1998) with scaling factor $f = 0.1$. Mantle lithosphere and sublithospheric flow is based on wet olivine (WOI, Karato and Wu, 1993) with scaling factors $f = 5$ (standard and upper cratonic mantle lithosphere), $f = 3$ (lower cratonic lithosphere), and $f = 1$ (sublithospheric mantle). These scalings are the same for Type I-III models. d) Strain softening of frictional-plastic rheology (yellow to red strength envelopes in panel c) is a function of total strain; a linear decrease of $\phi_{\text{eff}}(\varepsilon)$ from 15° – 2° over a strain range 0.5–1.5, where ε = second invariant of strain.

dome (Fig. 4b) is also similar to the Fitz and Mann (2013b, Fig. 2 panel b) conceptual model. The surrounding crust has subsided anomalously forming sag basins (Kusznir and Karner, 2007), which is also consistent with lower crustal flow toward and into the core complexes (Fitz and Mann, 2013a, 2013b). For these reasons we believe that some Type II margins will be shown to contain core complexes, like those in extended backarc regions, e.g. the Aegean Sea (Lister et al., 1984; Jolivet et al., 2010) and possibly in the South China Sea (Savva et al., 2013; Li et al., 2014).

3. Model design (see Appendix A for details)

We use finite-element models (Sopale, Fullsack, 1995) to calculate upper-mantle thermo-mechanically coupled, plane-strain, incompressible viscous-plastic creeping flows using an Arbitrary

Lagrangian-Eulerian (ALE) method. The model design (Fig. 2) shows the configuration of the $1200 \times 600 \text{ km}$ A and C models.

When stress is below yield, power-law flow is based on laboratory experiments. Effective viscosity is specified by:

$$\eta = f A^{-1/n} (\dot{\jmath}_2')^{(1-n)/2n} \exp \left[\frac{Q + Vp}{nRT} \right] \quad (1)$$

where $\dot{\jmath}_2'$ is the second invariant of the deviatoric strain rate tensor $\frac{1}{2}\dot{\varepsilon}_{ij}'\dot{\varepsilon}_{ij}'$, n is the power-law exponent, A is the pre-exponential scaling factor, Q is the activation energy, V is the activation volume, p is the pressure, T is the absolute temperature and R is the universal gas constant. A , n , Q and V are derived from laboratory experiments and the parameter values are listed in Table 1. The factor f is used to scale viscosities calculated from the reference quartz, dry Maryland diabase and olivine flow laws, thereby

Table 1
Model parameter values.

Parameter	Symbol	Value
<i>Rheological parameters</i>		
Angle of internal friction	$\phi(\varepsilon)$ and strain range of softening, ($\varepsilon = I_2'$)	15°–2°, 0.5–1.5
Cohesion		
Wet Quartz (Gleason and Tullis, 1995)	C	0 Pa
Power law exponent	n	4.0
Activation energy	Q	223×10^3 J/mol
Initial constant ^a	A	1.10×10^{-28} Pa ⁻ⁿ /s
Activation volume	V	0 m ³ /mol
Crust scaling factor (Types I, II, C)	f _c	30, 0.02, 100
<i>Dry Maryland Diabase</i> (Mackwell et al., 1998)		
Power law exponent	n	4.7
Activation energy	Q	485×10^3 J/mol
Initial constant ^a	A	5.77904×10^{-27} Pa ⁻ⁿ /s
Activation volume	V	0 m ³ /mol
Lower crust scaling factor (Type III)	f _{lc}	0.1
<i>Wet Olivine</i> (Karato and Wu, 1993)		
Power law exponent	n	3.0
Activation energy	Q	430×10^3 J/mol
Initial constant ^a	A	1.7578×10^{-14} Pa ⁻ⁿ /s
Activation volume	V	15×10^{-6} m ³ /mol
Mantle lithosphere scaling factor	f _{ml}	5
Sub lithosphere scaling factor	f _{sli}	1
Upper cratonic mantle lithosphere scaling factor	f _{ucm}	5
Lower cratonic mantle lithosphere scaling factor	f _{lcm}	3
Universal gas constant	R	8.3144 J/mol/°C
<i>Thermal parameters</i>		
Diffusivity	κ	1×10^{-6} m ² /s
Diffusivity sub lithospheric mantle	κ_{slm}	21.5×10^{-6} m ² /s
Diffusivity cratonic lithosphere mantle	κ_{cml}	2.24×10^{-6} m ² /s
Crustal radioactive heat production	A _R	0.9×10^{-6} W/m ³
Volume coefficient of thermal expansion	α_T	2×10^{-5} /°C
Surface temperature	T ₀	0 °C
<i>Standard lithosphere</i>		
Initial Moho temperature	T _m	550 °C
Base lithosphere temperature	T _l	1330 °C
<i>Cratonic lithosphere</i>		
Initial cratonic Moho temperature	T _{cm}	480 °C
Base cratonic lithosphere temperature	T _{cml}	1380 °C
Basal temperature	T _a	1520 °C
<i>Densities</i> (T ₀ = 0 °C)		
Crustal density	$\rho_c(T_0)$	2800 kg/m ³
Mantle lithosphere density	$\rho_m(T_0)$	3300 kg/m ³
Sub lithospheric mantle density	$\rho_a(T_0)$	3300 kg/m ³
Upper cratonic mantle lithosphere density	$\rho_{ucm}(T_0)$	3283 kg/m ³
Lower cratonic mantle lithosphere density	$\rho_{lcm}(T_0)$	3285 kg/m ³
<i>Dimensions and boundary condition</i>		
Base of crust (Types I–III)		35 km
Thickness of lower crust (Type III)		10 km
Base mantle lithosphere		125 km
Base cratonic mantle lithosphere		250 km
Base upper mantle		600 km
Extension velocity	V/2	0.75 cm a^{-1} (half rate)
Top boundary condition		Stress free surface
Side boundary conditions		Free slip, normal velocity V
Basal boundary conditions		Free slip, zero normal velocity

^a Values of A have been converted from the experimental values to values appropriate for tensor invariant conditions.

producing strong and weak versions of these materials (Fig. 2, caption, Table 1, Appendix A, Methods). Frictional-plastic (Drucker–Prager) yielding occurs when:

$$\sigma_y = (J'_2)^{1/2} = C \cos \phi_{eff} + p \sin \phi_{eff} \quad (2)$$

where $J'_2 = \frac{1}{2}\sigma'_{ij}\sigma'_{ij}$ is the second invariant of the deviatoric stress, ϕ_{eff} is the effective internal angle of friction, C is cohesion, and $p \sin \phi_{eff} = (p - p_f) \sin \phi$ for pore fluid pressure p_f . This approximates frictional sliding in rocks, including pore-fluid pressure effects. Strain softening is introduced by a linear decrease of $\phi_{eff}(\varepsilon)$ from 15° to 2°, over the range of strain ε 0.5–1.5 (Fig. 2, Appendix A, Methods and Table 1). $\phi_{eff}(\varepsilon) \approx 15^\circ$ corresponds to hydrostatic pore pressure. Nominal strength envelopes (Fig. 2c) are

shown in the initial and strain-softened states. The strengths are designed to achieve strong frictional-plastic crust for Type I and craton crusts, and a viscously weak lower crust in Type II, which contrasts with the strong frictional-plastic lower crust in Type III.

The initial temperature for A models is laterally uniform, includes radioactive heat production in the crust ($A_R = 0.9 \mu\text{W m}^{-3}$) and has basal heat flux ($q_m = 19.5 \text{ mW m}^{-2}$). The sides are insulated. In C models the craton has a reduced geothermal gradient, and low surface heat flow. The gradient is adiabatic in the sublithospheric mantle. Cratonic mantle lithosphere is compositionally depleted such that the upper and lower parts have $\rho_m(T_0) = 3283 \text{ kg m}^{-3}$ (density anomaly, -17 kg m^{-3}) and $\rho_m(T_0) = 3285 \text{ kg m}^{-3}$ (density anomaly, -15 kg m^{-3}). Mechanical

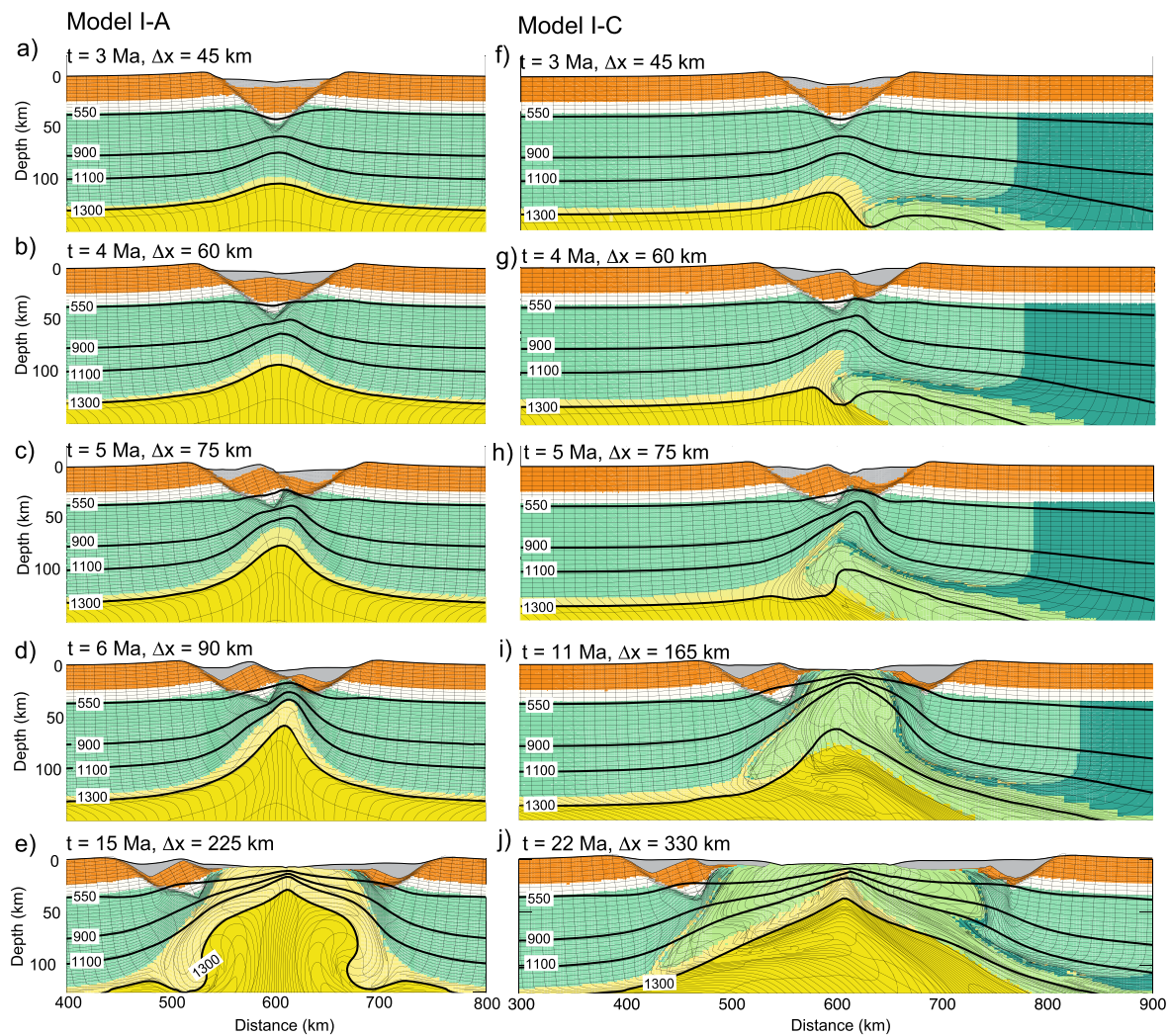


Fig. 3. Evolution of Models I-A (panels a–e) and I-C (panels f–j) (shown for a sub-region of the model domain). t = time since onset of extension, Δx = total extension at uniform velocity 1.5 cm a^{-1} . Contours are isotherms in $^{\circ}\text{C}$. Sediments (grey), upper/mid crust (orange), lower crust (white), continental mantle lithosphere (green), cratonic upper mantle lithosphere (dark green), cratonic lower mantle lithosphere (lightest green), oceanic lithosphere (pale yellow), asthenosphere (yellow). Information on the distribution of thinning factors for the upper and lower crust can be estimated from their initial thickness divided by their current thickness.

and thermal systems are coupled and are solved sequentially at each time step.

4. Model explanation of Type I margins: depth-dependent extension with strong crust bonded to mantle

We suggest that characteristics of Type I margins, noted above, are explained by reference to Models I-A/C (Fig. 2). The crust and uppermost mantle lithosphere are strongly bonded and undergo frictional-plastic (FP) brittle deformation while the lower lithosphere deforms by viscous (V) power-law, ductile flow. Depth-dependent extension is a consequence of this two-layer rheology. Fig. 3 contrasts results when the rift is underplated by asthenosphere (I-A) or cratonic lower lithosphere (I-C).

Both models share the following phases of evolution. 1) Symmetric conjugate FP faulting/shearing of the upper layer defining a subsiding keystone crustal block, which is underlain by a necking ductile lower lithosphere layer (Figs. 3a, f). 2) Asymmetric simple shear extension resembling conceptual upper- and lower-plate conjugate margins (Wernicke, 1985; Lister et al., 1991) (Figs. 3c, h), caused by positive feedback during strain softening, which preferentially weakens one of the conjugate shear zones bounding the keystone block. This shear then dominates. 3) Rupture of the crust

during exhumation of the lower lithosphere along the dominant weak shear (Figs. 3d, i), which acts as a simple shear detachment (Wernicke, 1985) rooting in the ductile mantle (Lister et al., 1991), and results in lithosphere-scale asymmetry. Small variations in conditions make the asymmetry more or less pronounced.

In both models the crust ruptures before the lower lithosphere and there is minor exposure of upper lithospheric mantle in the narrow distal margins. However, the major contrast is underplating in I-C by an up to 75 km thick layer of lower cratonic lithosphere, which is subsequently exposed and then progressively rifted to form symmetric 150 km wide zones (ZECM, zone of exposed continental mantle) in both distal margins (Figs. 3i, j). Production of normal oceanic lithosphere is therefore delayed, which has implications for magma generation. Asthenospheric decompression melting will occur as asthenosphere upwells beneath the cratonic underplate, particularly where this layer is thinner than 60 km. Basalt magma may underplate, intrude, or erupt through the exhumed continental lithosphere potentially representing significant addition of melt adjacent to the true oceanic crust even at magma-poor margins. The resultant magnetic anomalies in the ZECM will be syn-rift in age, significantly older (possibly many millions of years) than final breakup and onset of production of normal

oceanic crust (Bronner et al., 2011). In summary, lower lithosphere counterflow produces a major difference in the transition region of the outer continental margin (I-C versus I-A, Fig. 3) and exhumes serpentinized, magma-impregnated continental mantle lithosphere (ZECM).

5. Comparison of Models I-A/C with the Newfoundland–Iberia conjugate margins

That Model I-A is compatible with the final phase of rifting of Newfoundland from Iberia was explained by Huismans and Beaumont (2011) by comparison with the observations and inferred evolution (Péron-Pinvidic and Manatschal, 2009; Sutra et al., 2013). The common Type I characteristics are (1)–(6) listed above, in particular: 1) major conjugate basin forming faults/shears forming a keystone and penetrating to the mid/lower crust, and 2) narrow transitional regions (<100 km wide) of crustal thinning. From this comparison Huismans and Beaumont (2011) concluded that the fundamental style of Type I margins occurs because the lithosphere is a strong bonded frictional-plastic entity with ductile deformation restricted to the lower mantle lithosphere. Equivalent, less extreme models will give similar results provided decoupling in the crust is limited. An essential requirement is a style of depth-dependent extension in which the upper layer (crust and uppermost mantle) ruptures before the lower layer (lower mantle lithosphere). This allows continental mantle lithosphere to be exhumed and exposed in narrow zones. This style is achieved in the model by early excision of lower crust and uppermost mantle, which places upper/mid-crust allochthons in direct contact with stretched mid/lower mantle lithosphere. When the crust ruptures this mantle lithosphere is exposed (Figs. 3d, e). The final stage is rupture of the mantle lithosphere and onset of sea-floor spreading.

An additional mechanism is required to produce wide zones of exhumed continental mantle as observed in some parts of the Newfoundland–Iberia margins (Fig. 1) (Dean et al., 2000; Minshull et al., 2001; Whitmarsh et al., 2001; Funck et al., 2003; Sutra et al., 2013). Model I-A does not exhume continental mantle as envisaged in the conceptual Sibuet and Tucholke (2013, Fig. 10), whereas cratonic underplating, Model I-C, does (Figs. 3i, j). In the Newfoundland case the counterflow probably comprises thick depleted mantle lithosphere, perhaps arc-type, as demonstrated by Beaumont and Ings (2012), not cratonic lithosphere.

Models I-A/C also reproduce many characteristics of the conjugate Labrador Sea margins between the Archean Nain province and the North Atlantic Craton, southwest Greenland. These are also narrow margins, with one rifting phase, and are possibly a better Type I archetype than the more complex two-phase, Jurassic and Cretaceous, Newfoundland–Iberia margins. Crust on the Labrador side thins to less than 10 km over a distance of 100 km (Chian et al., 1995, Fig. 12) and the conjugate Greenland margin is less than 50 km wide (Chalmers et al., 1993; Chian et al., 1995, Fig. 12). Further north, offshore the Torngat Orogen, crust thins from 38 km to less than 10 km over a distance of only 25 km (Funck and Louden, 1999, Line 5E, Fig. 13; Keen et al., 2012). Xenolith studies (e.g. Sand et al., 2009) confirm the cratonic nature of lithosphere beneath southwest Greenland with a depleted upper mantle and low heat flux. In this case the existence of serpentinized mantle beneath the margins is inferred from seismic evidence (Chian et al., 1995) and is therefore not proven. The subsidence of the proximal Labrador margin is also consistent with depth-dependent extension in which thinning of the lower lithosphere is much greater than that of the crust (Royden and Keen, 1980), as is also seen beneath the rotated fault block Models I-A/C (Figs. 3d, i).

6. Model explanation of Type II margins: 1) depth-dependent extension with weak lower crust

We suggest that characteristics of Type II margins, as noted above (Fig. 1e), are consistent with Models II-A/C (Fig. 4). The style of depth-dependent extension is totally different from Models I-A/C now that there is widespread viscous horizontal decoupling between the upper and lower lithosphere, not strong bonding.

The extension style is determined by the respective long and short necking length scales of the crust and mantle lithosphere. Mantle lithosphere necking is similar to Models I-A/C, but crust extends over a much larger scale because it decouples from the mantle far into the continent (Fig. 4).

A characteristic of Models II-A/C with very low viscosity lower crust is that extension of the upper crust is accompanied by gravitational extrusion of the lower crust as a channel flow into the extending regions. Lateral transfer of lower crust and its exhumation into the upper crust as core complexes (Whitney et al., 2013) (Figs. 4e, f, g) results in protracted crustal extension, leading to ultra-wide margins and delayed crustal breakup. The cross-sectional area balance of the wide margin crust is achieved by alternating regions where lower crust flows into the core complexes juxtaposed against boudins/rafts of relatively unextended upper crust (Fig. 4e). Core complexes are ubiquitous in our models with a weak crust (cf. Beaumont and Ings, 2012; Models 3 and 5). Even the thin, ‘hyperextended’, distal region may contain core complexes. Core complexes would be even more prominent if we included the effects of melting on the crustal rheology and density (e.g. Rey et al., 2009; Schenker et al., 2012). In Models II-A/C lower crust flows rapidly to fill the accommodation space between upper-crustal boudins as they develop, and faster than sediment fills this space. In natural systems core complexes may develop more slowly than in Fig. 4, but we suspect that Type II continental margins contain core complexes, although they are not recognized in current compilations (Whitney et al., 2013, Fig. 2).

Models II-A and II-C have similar ultra-wide continental margins, but differ in regard to underplating by asthenosphere (II-A) versus cratonic mantle lithosphere (II-C). Counterflow of cratonic lithosphere in Model II-C is equivalent to that in Model I-C but the two models contrast because the margin crust is narrow in I-C, thereby exposing counterflowed mantle lithosphere, whereas the margin crust is very wide in II-C and the counterflow underplates it but is not exposed at the seafloor. Depending on the buoyancy of the underplating counterflow the underplated crust in II-C may subside less than its counterpart in II-A (Huismans and Beaumont, 2011).

The implications for magma generation and the thickness of the initial oceanic crust are therefore different at Type II-C margins and Type I-C margins, where in the latter counterflowed continental lower lithosphere may inhibit decompression melting or absorb melts (Section 4). This will only happen at Type II-C margins if the length-scale of the counterflow is sufficient to underplate the rift axis at the time of final breakup. If not decompression melting and oceanic crust production should be normal at both Type II-A and II-C following breakup.

7. Model explanation of Type III margins: 2) depth-dependent extension with strong lower crust

In Type II margins removal of lower crust is explained by lateral flow. However, lower crust can alternatively be removed by advection out of the rift zone with the mantle, as demonstrated by Models III-A/C (Fig. 5). In this mechanism decoupling occurs at the base of the middle crust while the lower crust remains strongly coupled to the mantle. Models II and III both allow decoupling between the crust and mantle lithosphere, but at a different

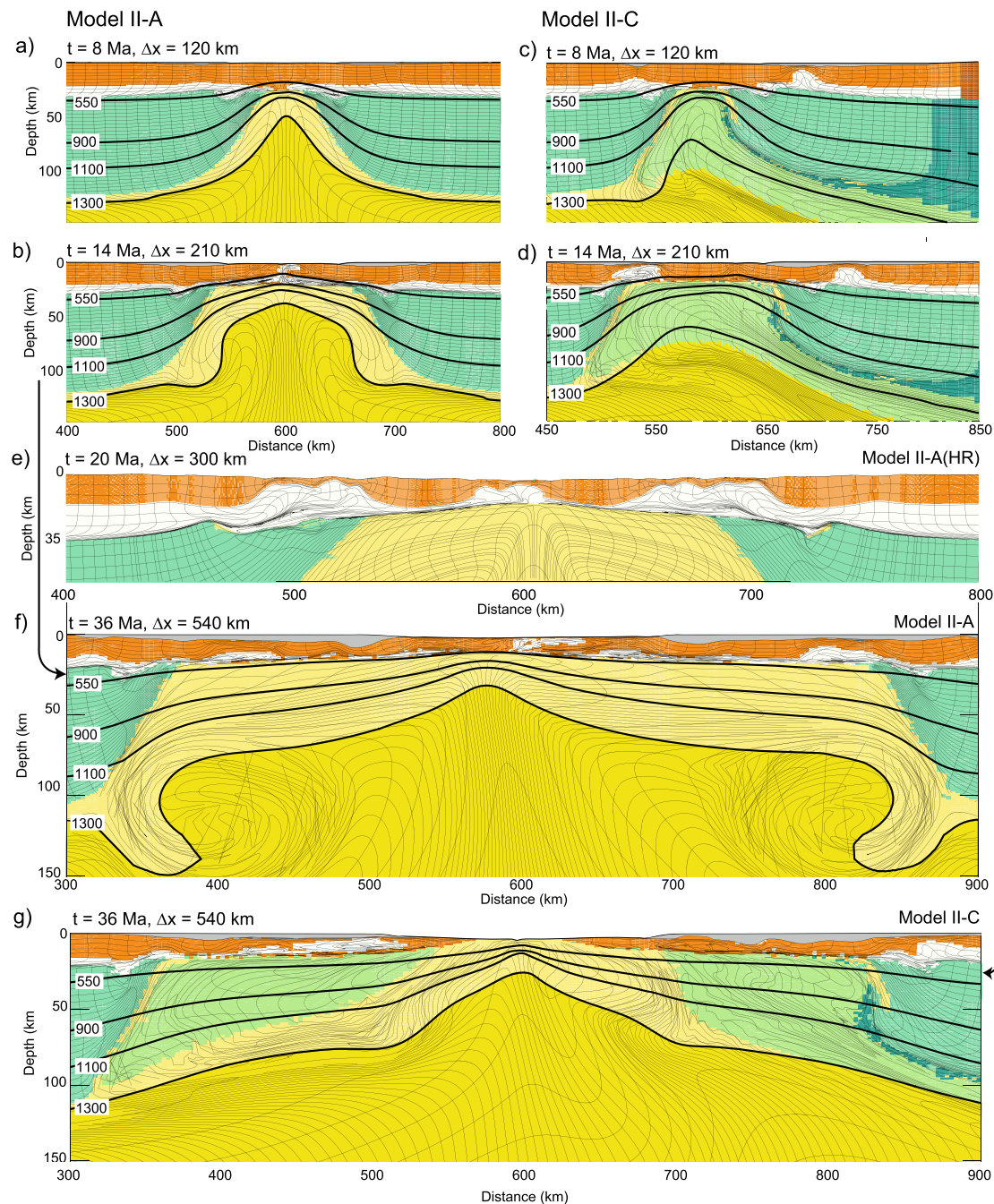


Fig. 4. Evolution of Models II-A (panels a, b and f), II-C (panels c, d and g), and II-A(HR) (panel e). e) Model II-A(HR) is a high resolution model with crust WQz xf , $f = 0.1$ which illustrates that core complexes even develop for higher crustal strength values. t = time since onset of extension, Δx = total extension at uniform velocity 1.5 cm a^{-1} . Contours are isotherms in $^{\circ}\text{C}$. Sediments (grey), upper/mid crust (orange), lower crust (white), continental mantle lithosphere (green), cratonic crust (brown), cratonic upper mantle lithosphere (dark green), cratonic lower mantle lithosphere (lightest green), oceanic lithosphere (pale yellow), asthenosphere (yellow). Lower panels correspond to models close to final breakup. Information on the distribution of thinning factors for the upper and lower crust can be estimated from their initial thickness divided by their current thickness.

level. Lateral advection of lower crust coupled to the mantle lithosphere may represent a third style of continental margin, Type III, in which the lower crust is missing. Currently, we are not aware of any margin where this style can be proven.

Models III-A/C extension consists of two phases. The first comprises early distributed stretching of the mid/upper crust, matched by concomitant rapid necking of lower crust and mantle lithosphere with a short length scale (Figs. 5a, c). Phase one ends with breakup of the mantle lithosphere while the upper lithosphere, which has decoupled over a wide region, is still extending with

relatively little thinning (Figs. 5a, c). In phase two lower crust and mantle lithosphere are efficiently advected away, without deformation, by the plate motion and a widening zone of asthenosphere or cratonic underplate upwells and is in direct contact with the extending mid/upper crust (Figs. 5e, f). This helps maintain a high temperature and the crust continues to extend, producing the ultra-wide margin. Phase two ends when crustal extension becomes focused in the distal margin leading to necking and final breakup (Figs. 5e, f). The implication for magmatism is similar to that of Type II margins with normal production of oceanic crust

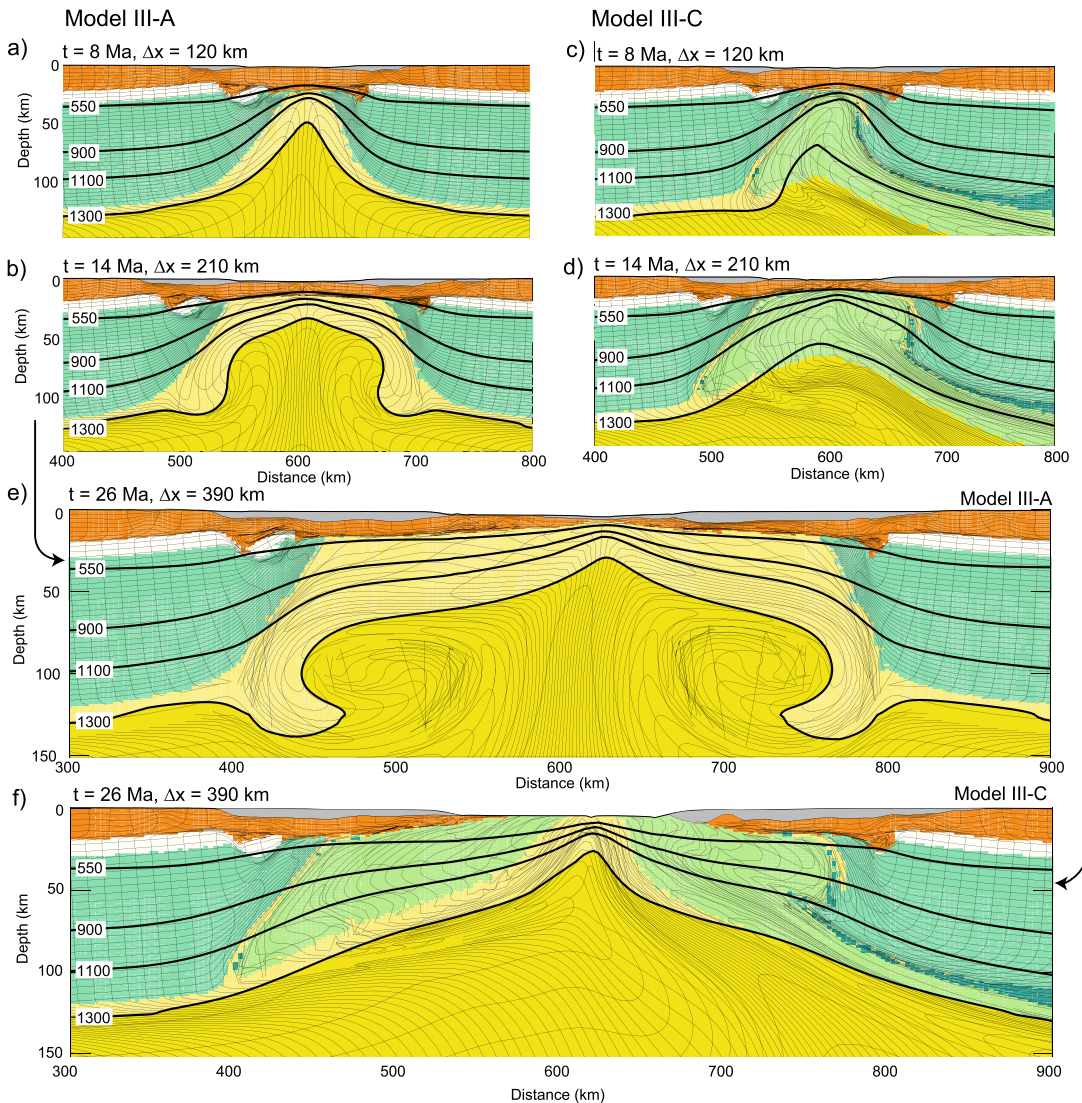


Fig. 5. Evolution of Models III-A (panels a, b and e) and III-C (panels c, d and f). t = time since onset of extension, Δx = total extension at uniform velocity 1.5 cm a^{-1} . Contours are isotherms in $^{\circ}\text{C}$. Sediments (grey), upper/mid crust (orange), lower crust (dry Maryland Diabase, $f = 0.1$) (white), continental mantle lithosphere (green), cratonic lower mantle lithosphere (lightest green), oceanic lithosphere (pale yellow), asthenosphere (yellow). Note exhumation of depleted lower mantle lithosphere in Model III-C at breakup (panel f). Information on the distribution of thinning factors for the upper and lower crust can be estimated from their initial thickness divided by their current thickness.

after final breakup of the continental crust unless the counterflowed cratonic lithosphere, in Type III-C, underplates the rift axis at breakup.

8. Comparison of Models II- and III-A/C with central South Atlantic ultra-wide margins

Comparison of Models II-A and III-A with observations from the ultra-wide central South Atlantic margins (Figs. 1e, f) indicates the following characteristics in common: ultra-wide strongly attenuated crust; wide regions of sag basin subsidence; sag basin subsidence even in areas where there is apparently little crustal extension; no evidence of lower crust; late syn-rift shallow water conditions, followed by large post-rift subsidence, suggestive of subsidence owing to asthenospheric cooling in nature, and produced in this way in the models, and; no flank uplifts. This comparison corresponds to the one in Huismans and Beaumont (2011) which concluded that the fundamental style of Type II margins, and by implication the wide central South Atlantic margins, occurs because there is viscous decoupling between upper and lower lithosphere. Equivalent but less extreme models will give similar

results provided sufficient decoupling occurs between upper and lower lithosphere. The essential requirement is a style of depth-dependent extension in which the lower lithosphere is removed while the crust is still extending, thereby placing highly-stretched upper crust in direct contact with hot upwelled mantle (Figs. 4f, g). This allows formation of wide crustal rifted margins underplated either by asthenosphere (Type II/III-A) or counterflowed depleted mantle lithosphere (Type II/III-C). The final step is crustal breakup followed by sea-floor spreading.

The late synrift/early post rift of many central South Atlantic conjugate margins is characterized by a puzzling observation, that of lacustrine and shallow marine conditions. This requires an isostatic balance with sub-crustal material that is more buoyant, less dense, than upwelled asthenosphere. Huismans and Beaumont (2011) proposed that this material is hot depleted lower-cratonic lithosphere as in Models II-C and III-C (Figs. 4g, 5f), representing the case of rifting adjacent to a craton (e.g. the Congo craton next to the South Atlantic and the Pilbara craton next to the Exmouth Plateau). This will reduce the synrift subsidence. The reduction is modest for the models shown here with a small 15 kg m^{-3} com-

positional density anomaly, but increases to ~ 1.3 km when the anomaly is 25 kg m^{-3} , resulting in sub-areal conditions for the top surface of 5–8 km thick sedimentary sag basins during the first 20 Ma of their evolution. The reduction could be even more for strongly depleted continental mantle lithosphere (Beaumont and Ings, 2012).

Margin underplating by depleted continental counterflow, as in Models II/III-C, is consistent with the following observations: lithosphere with a high seismic shear wave velocity under the central South Atlantic rifted margin and ocean basin connected to the Congo craton that can be interpreted as having continental affinity (Begg et al., 2009), and; the relatively magma poor nature of this part of the South Atlantic margin. Direct evidence of underplating by depleted lower continental lithosphere is lacking, but if the flow were strong enough this material could be exhumed in the distal margin at the rift axis at the time of final crustal breakup, as in Type I-C models. Currently, the nature of the basement below the distal central South Atlantic margins is poorly constrained. Seismic reflection images from this region are suggestive of mantle exhumation (Unternehr et al., 2010), while refraction seismic analysis and gravity modelling suggests crustal densities (Contrucci et al., 2004).

In a different context, it is however worth noting that aspects of the active Woodlark Basin rift system, noted earlier, are very similar to Model II-A. In particular Model II-A (Figs. 4a, b) is very similar to a cartoon representing the lithospheric-scale structure below the D'Entrecasteaux islands (Eilon et al., 2014, Fig. 12) and brackets the estimated extension, 140–190 km at that location. The cartoon shows the same dramatic thinning/removal of the mantle lithosphere. The style of lateral flow and emplacement of the gneiss dome (Fig. 4b) is also similar to the Fitz and Mann (2013b, Fig. 2 panel b) conceptual model. That the surrounding crust has subsided anomalously forming sag basins (Kusznir and Karner, 2007), which is consistent with lower crustal flow toward and into the core complexes (Fitz and Mann, 2013a), was also noted earlier.

9. Discussion

9.1. Contrasting styles of extension and timing of lithospheric breakup

Our proposition is that Type I and Type II margins, and Type III if they exist, are a direct consequence of their respective lithospheric rheological properties, which lead to contrasting styles of depth-dependent extension. These styles, exemplified by Models I–III, can be readily understood by considering extension and necking of a laminate (Fig. 6). Here the food analogy is the layered chocolate-caramel bar. Type I is a strongly bonded laminate with a frictional plastic (brittle/chocolate) upper lithosphere underlain by a viscous (ductile/caramel) lower lithosphere (below dashed line Fig. 6a). During extension the upper lithosphere fails by faulting such that this layer ruptures and breakup occurs while the lower lithosphere is still necking viscously (Fig. 6a).

Types II and III differ from Type I in that they have an additional weak viscous (ductile/caramel) filling layer in the crust. This filling may be lower crust (Type II, Figs. 6c, d, white color layer) or mid-crust (Type III, Figs. 6e, f, lower orange layer). This low viscosity layer allows the upper lithosphere to decouple from the lower lithosphere over a wide region. During extension the lower lithosphere necks and ruptures in a similar manner to the Type I laminate. However, at the time it breaks up the upper lithosphere has thinned relatively little because its extension is distributed across such a wide region. Breakup of the upper lithosphere occurs much later after it has been stretched to form a wide thin layer bridging between the severed lower lithosphere conjugates. These now recede at the tectonic plate velocities without further deformation (Figs. 6c, e). In Type II the lower crust participates in

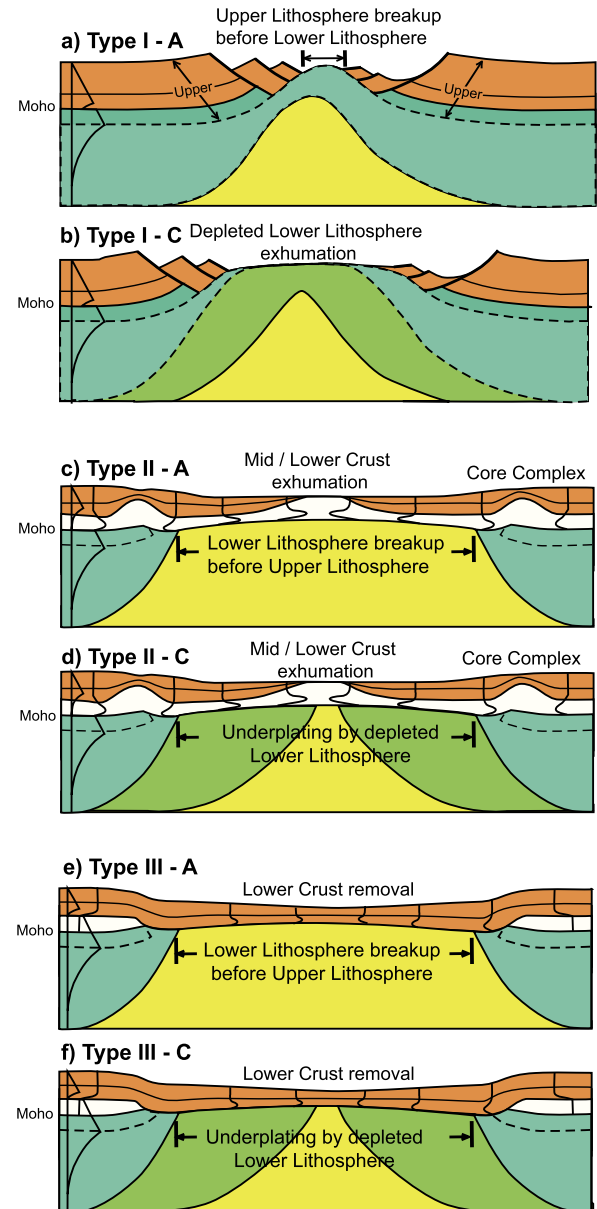


Fig. 6. Conceptual diagram illustrating the proposed contrasting extension, necking and breakup styles of Type I, II and III rifted margins. Each of these types is shown in pairs A and C to indicate underplating by asthenosphere or by depleted cratonic lower lithosphere.

the crustal extension and may form core complexes or flow to the rift axis, adjustments that may continue into the postrift, whereas in Type III lower crust is strong, remains bonded to the mantle lithosphere, and is transported away with it.

Type I and Types II/III, are therefore opposites in which upper lithosphere breakup occurs either significantly before or after lower lithosphere breakup (Fig. 6). The concept of different times of breakup of lower and upper lithosphere follows directly from the highly contrasting necking times and length scales of the upper and lower lithosphere, the 'Stiff' and 'Pliable' layers of Chenin and Beaumont (2013). Uniform extension (UE) is a special case for which the two breakup times coincide, but UE is unlikely for a rheologically layered lithosphere.

These concepts lead directly to the respective narrow and wide necking geometries of Type I and Type II/III margins. They also explain exhumation and exposure of a small region of continental mantle lithosphere (Type I-A, Fig. 6a), why this exhumation

is unlikely (Type II-A or III-A, Figs. 6b, c), and why lower crust and continental mantle lithosphere are missing under large areas of Type II/III margins.

Although small regions of continental mantle lithosphere may be exhumed in Type I-A margins, lower lithosphere counterflow is proposed as the mechanism that exposes much larger tracts in the distal regions of Type I margins (Fig. 6b). Whether similar exposure occurs at Type II/III margins depends on the length scale of the counterflow by comparison with the stretching length scale of the crust at breakup (Figs. 6d, f). By implication, lower continental lithosphere may underplate the extending crust, and be in direct contact with it, even if it is not exposed.

We note that Models I-A/C, II-A/C, and III-A/C were purposely chosen to be end-member examples with strongly contrasting rheological properties. Margins with intermediate properties certainly exist but our purpose is to focus on the end-members. Intermediate styles will certainly result in Models II and III if the extension velocity is reduced sufficiently, such that the thinning crust cools enough that coupling occurs during rifting. Under these circumstances we expect a transition from Type II and III styles to Type I. We also note that conjugate margins can have very different styles, particularly where rifting occurs at the boundary between a stiff Archean craton and younger, pliable, lithosphere, which will tend to give one Type I conjugate and the other of Type II or III.

9.2. Templates for the development and subsidence of the associated sedimentary basins

One test of the applicability of the models is that the characteristics of sedimentary basins predicted on the basis of the models should agree with observations from these three types of margins. We therefore describe the associated basin characteristics in terms of zonal templates and present them as testable model predictions. To limit the length of this section we focus on Models I-A to III-A and then discuss the effects of cratonic underplating.

We divide the model margins (Figs. 7–9) into Proximal (P), Mid (M) or Sag (S), and Distal (D) zones and describe the unloaded subsidence characteristics of each of these regions during the syn-rift and post-rift phases. We focus on the diachronous evolution shown as a simplified two phase (Early, E and Late, L) synrift space-time diagram, followed by a postrift phase (P). The template accounts for where and when extension occurs, the effect of this extension on subsidence/uplift and accommodation, and the implications for faulting of the sediments in the basins.

9.2.1. Sedimentary basin template for Type I margins

End-member Model I-A margins are typically narrow, with narrow P, M and D zones (Fig. 7). The timescale for rifting and breakup is significantly shorter (10–20 Ma, depending on the rifting velocity) than that for Model II-A margins (30–40 Ma) and occurs with less extension. The unloaded subsidence (Fig. 7) shows only flexural rift flank uplift for P because lithosphere is not stretched beneath P. The flank uplift, as seen in Models I-A/C (Fig. 3), will persist until it is eroded. There may, however, be offset rift basins (not shown) in the adjacent continental interiors (Chenin and Beaumont, 2013). The small-scale convection seen below the rift flanks hardly contributes to their uplift in any of the models.

At the scale of the margin the crust and uppermost mantle extend together in zones M and D. Detachment and disaggregation of crustal blocks is mainly limited to the vicinity of the crustal keystone (Model I-A/C, Fig. 3) but will be distributed across a wider region in less end-member cases. This implies that M will be characterized by fault blocks and rift basins during the E synrift, followed by a diachronous decrease in rate of extension in the L synrift if keystone disaggregation focuses in the distal margin (Fig. 7).

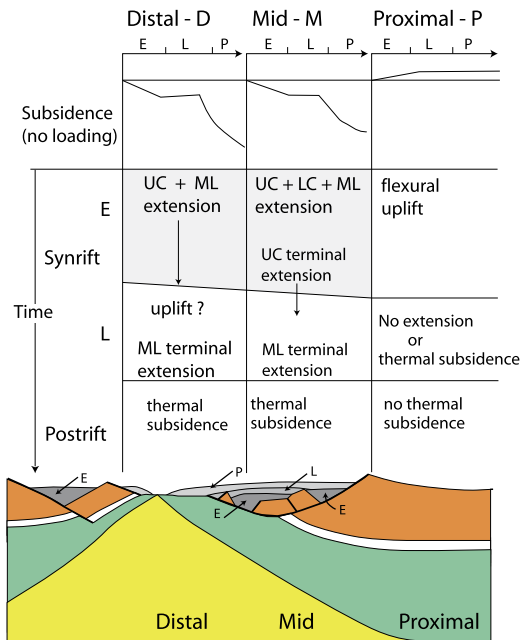


Fig. 7. Template for the evolution of Model I-A margins and associated sedimentary basins. Upper panel shows diagrammatic unloaded subsidence characteristics of Distal, Mid and Proximal regions of the margin during Early synrift (E), Late synrift (L) and Postrift (P). Middle panel is a space-time diagram showing location of extension (UC Upper Crust, LC Lower Crust, ML Mantle lithosphere) during the E and L synrift and postrift phases. This part of the diagram can be interpreted as showing the successive processes (top to bottom of columns) leading to subsidence/uplift that would be seen by an observer in each of the Distal, Mid and Proximal zones. Horizontal scans of the columns show relative behaviors at equivalent times. This means that tilted lines indicate diachronous evolution. Lower panel shows diagrammatic interpretation of the model margin characteristics with sediments labeled E (Early synrift), L (Late synrift) and P (Postrift).

Lower mantle lithosphere thinning lags E synrift crustal extension in M but persists during the L synrift. This means that rapid E synrift subsidence in M may become muted in the L synrift. Thermal subsidence, and development of sag basins, could start in M before final lower lithosphere breakup if L synrift lower lithosphere stretching focuses in D. However, this will be difficult to detect because the synrift phases are short and diachroneity limited.

D, the distal outer margin, experiences crustal and uppermost mantle extension throughout the synrift terminating in breakup of the crust. Subsidence is in proportion to crustal thinning, offset by thinning of the lower mantle lithosphere and replacement by hot asthenosphere. A subsidence hiatus or even uplift may occur after crustal breakup while the lower mantle lithosphere is still extending and thinning. Thermal subsidence starts in the postrift.

9.2.2. Sedimentary basin template for Type II margins

Model II-A margins are wide and the syn-rift phase is long (30–40 Ma, depending on the rifting velocity), long enough for the diachronous evolution to be recognized in extension and faulting of the crust, and in the differing subsidence of P, S and D. P develops rift basins and limited syn-rift subsidence because the crust decouples and stretches well into the continent. There is no postrift subsidence because the mantle lithosphere in this region is not thinned.

S is a wide zone with characteristic sag basins. It experiences E synrift crustal extension and subsidence, but less L synrift subsidence because crustal extension migrates diachronously into the distal margin. S may experience a hiatus in subsidence or transient uplift as the continental mantle lithosphere is pulled from beneath this region later in the synrift and this is followed by thermal subsidence, notably starting in the L synrift. Removal of

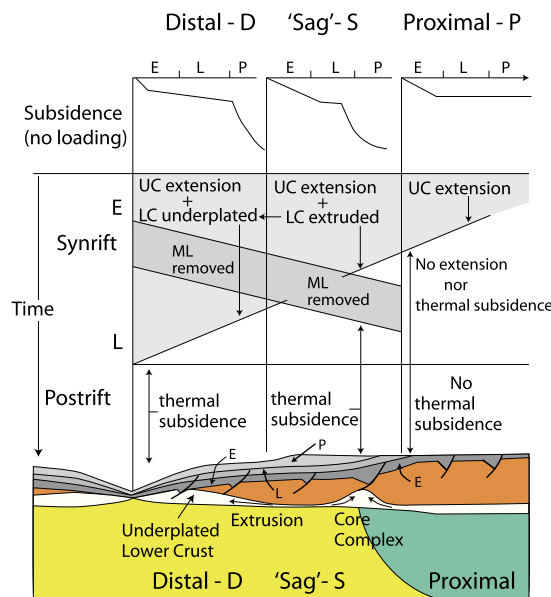


Fig. 8. Template for the evolution of Model II-A margins and associated sedimentary basins. Upper panel shows diagrammatic unloaded subsidence characteristics of Distal, Sag and Proximal regions of the margin during Early synrift (E), Late synrift (L) and Postrift (P). Middle panel is a space-time diagram showing location of extension and extrusion (UC Upper Crust, LC Lower Crust, ML Mantle lithosphere) during the E and L synrift and Postrift phases. This part of the diagram can be interpreted as showing the successive processes (top to bottom of columns) leading to subsidence/uplift that would be seen by an observer in each of the Distal, Mid and Proximal zones. Horizontal scans of the columns show relative behaviors at equivalent times. This means that tilted lines indicate diachronous evolution. Lower panel shows diagrammatic interpretation of the model margin characteristics with sediments labeled E (Early synrift), L (Late synrift) and P (Postrift).

mantle lithosphere is also diachronous but occurs in the opposite sense to crustal extension (Fig. 8).

Crust in D experiences extension throughout the synrift terminating in breakup. It is the first zone to experience uplift, or a hiatus in subsidence, owing to the diachronous removal of the continental mantle lithosphere. Thermal subsidence, from asthenospheric cooling, may therefore start earlier in D than beneath S, and can occur while the most distal crust continues to stretch.

E synrift crustal extension is distributed across the entire margin. Therefore crust and sediments experience E synrift faulting in all zones. However, P and S will not undergo faulting in the L synrift owing to the diachronous migration of extension into D. This means that early sag basin sediments are predicted to be faulted but not their late synrift sediments. Faulting in distal margin sediments will continue until crustal breakup.

An additional complication, shown in a simplified way (Fig. 8 bottom), is the possibility of the raft and core complex style of extension seen in Models II-A/C, which will modify the distribution of crustal deformation and the associated subsidence. The effect is clearly seen in Fig. 4e where the rafts of upper continental crust (orange) have suffered relatively little internal extension and faulting. Instead, extension is achieved by boudinage, which separates the rafts and leaves only a very thin carapace of upper crust. The gaps formed in this way are synchronously filled with laterally flowed and exhumed lower crust (white) that forms core complexes. Under these circumstances it is the detachment faults bounding the core complexes that accommodate most of the extension. Sag basins will develop above the rafts of upper crust because the rafts will sink where lower crust beneath them is withdrawn to be extruded into the core complexes. Equivalent sag basins will develop above the core complexes if the core complexes have accommodation space above them. This will depend on competition between lower crustal flow into the core complex

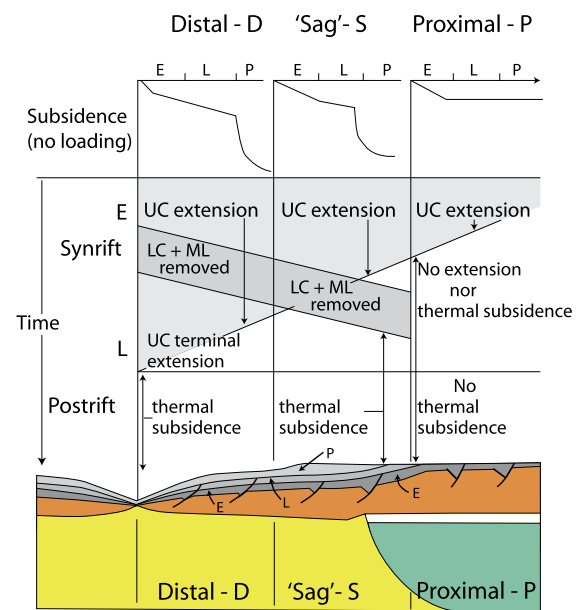


Fig. 9. Template for the evolution of Model III-A margins and associated sedimentary basins. Upper panel shows diagrammatic unloaded subsidence characteristics of Distal, Sag and Proximal regions of the margin during Early synrift (E), Late synrift (L) and Postrift (P). Middle panel is a space-time diagram showing location of extension and advective removal (UC Upper Crust, LC Lower Crust, ML Mantle lithosphere) during the E and L synrift and Postrift phases. This part of the diagram can be interpreted as showing the successive processes (top to bottom of columns) leading to subsidence/uplift that would be seen by an observer in each of the Distal, Mid and Proximal zones. Horizontal scans of the columns show relative behaviors at equivalent times. This means that tilted lines indicate diachronous evolution, in particular the removal of the lower crust and lithospheric mantle. Lower panel shows diagrammatic interpretation of the model margin characteristics with sediments labeled E (Early synrift), L (Late synrift) and P (Postrift).

and sedimentation. Vigorous flow may even produce subaerial core complexes, whereas slow flow will result in more accommodation space with the potential to develop thick sag basins. In summary, the raft and core complex style of extension creates sag basins by removing lower crust and emplacing it into core complexes.

9.2.3. Sedimentary basin template for Type III margins

Model III-A margins are similar to Model II-A margins except that lower crust is totally removed from beneath the D and S zones by diachronous translation (Fig. 9). Characteristics of zone P are the same as in Model II-A. Subsidence of S and D is now linked to the combination of upper crustal extension, which migrates diachronously toward the distal margin, and the timing of the oppositely vergent diachronous removal of lower crust and continental mantle lithosphere and their replacement by upwelled hot asthenosphere. Total removal of lower crust will enhance subsidence of the sag basins by comparison with Model II-A margins (Fig. 8), but the influx of hot asthenosphere will again temporally offset this enhancement, possibly leading to a wave of uplift propagating from D to S. Subsidence will restart by diachronous thermal cooling because emplacement of hot asthenosphere is also diachronous, beginning in the L synrift. In summary, subsidence of S is potentially complex with upper crust extension and associated subsidence waning after the E synrift, followed by limited subsidence or a hiatus during removal of lower crust and mantle lithosphere, and then the onset of thermal subsidence. This means that sag basins may evolve for more than 20 Ma during the syn-rift, show no evidence of extension after the E synrift, and begin thermal subsidence during the L synrift before final crustal breakup in D.

9.2.4. Effect of underplating by lower lithosphere counterflow on sedimentary basin subsidence

The primary effect of underplating by depleted continental mantle lithosphere as opposed to asthenosphere is to increase the duration of the synrift, by up to 20 Ma, because ‘synrift’ must now include the rifting and breakup of the underplated continental mantle lithosphere before the onset of oceanic spreading. The time available for development and subsidence of synrift sedimentary basins is correspondingly increased significantly and extension in S and D may continue during rifting of the continental margin underplate.

Correspondingly, template I-C (a modified version of Fig. 7) must include a zone, ‘C’, outboard of D, where the continental mantle is exhumed and rifted, and the L synrift must be extended to include the time taken to rift C. Templates II-C and III-C (modified versions of Figs. 8 and 9) may also require the extended L synrift and zone C if continental mantle lithosphere is exhumed in the distal margin.

Counterflow also modifies margin subsidence. Counterflow is only efficient when the lower continental mantle lithosphere is less dense than the upwelling asthenosphere. It follows that regions that are underplated by the counterflow will initially subside less than those underplated by asthenosphere (Huismans and Beaumont, 2011; Beaumont and Ings, 2012). The decrease depends on the density anomaly of the depleted underplate ($10\text{--}80 \text{ kg m}^{-3}$) and its thickness (up to 75 km). The discussion in Huismans and Beaumont (2011, Supplementary Information, part 4) also applies here because the models have similar properties. Reduced subsidence has the potential to keep the sag basins, zone S, sub-aerial during the synrift. However, it may only be temporary if there is pervasive refertilization of the underplated continental mantle lithosphere by melts and other fluids when asthenosphere upwells later in the rifting process (Müntener et al., 2010; Müntener and Manatschal, 2006; Beaumont and Ings, 2012). Such refertilization can potentially increase the density to that of fertile mantle.

10. Conclusions

We have identified and listed characteristics of two end-member types of rifted continental margin, Types I and II (Fig. 1), and argue these characteristics are not explained by uniform extension of the lithosphere (McKenzie, 1978). Instead, we interpret them in terms of depth-dependent extension and present dynamical models of lithospheric extension that reproduce these characteristics as exemplified by the narrow Newfoundland–Iberia and ultra-wide South Atlantic type examples. On the basis of the dynamical models we develop simple conceptual model descriptions of Type I and II margins. The pivotal difference is that in Type I upper lithosphere breakup occurs while the lower lithosphere is still necking, whereas in Type II the upper lithosphere extends over a wide region resulting in distributed necking and thinning leading to breakup long after that of the lower lithosphere. The models and associated concepts are consistent with a list of characteristics of these margins. A particular test is that the models should also explain the subsidence history of the associated sedimentary basins and we have presented templates for these characteristics emphasizing the zonation and diachronous development.

The inferred absence of lower continental crust beneath some Type II margins can be explained by Models II-A/C, which show its absorption into the upper crust as metamorphic core complexes during extension. An alternative mechanism for removal of lower crust is that it both rifts and is transported with the underlying mantle lithosphere from beneath the margin, as proposed for Type III margins and shown by Models III-A/C.

We also propose that exhumation of large tracts of continental mantle in outer continental margin transition zones is the result of lower continental mantle lithosphere counterflow during rifting, A versus C models. This flow is most likely where the rift is bordered by thick, depleted, low density cratons but may also occur for younger depleted arc-type lithosphere.

Acknowledgements

RH was funded by University of Bergen and by the Research Council of Norway. CB was funded by an NSERC Discovery Grant (48-2012), and the Canada Research Chair in Geodynamics. Numerical models used the software SOPALE, originally developed at Dalhousie University by P. Fullsack. This version was further enhanced by D. Guptill and members of the Dalhousie Geodynamics Group. We thank Taras Gerya and an anonymous reviewer for their reviewers. We also thank Janice Allen for contributing the model result shown in Fig. 4e.

Appendix A. Supplementary material

Supplementary material related to this article can be found online at <http://dx.doi.org/10.1016/j.epsl.2014.09.032>.

References

- Aslanian, D., Moulin, M., Olivet, J.-L., Unternehr, P., Matias, L., Bache, F., Rabineau, Nouzé, H., Klingelhoefer, F., Contrucci, I., Labails, C., 2009. Brazilian and African passive margins of the Central Segment of the South Atlantic Ocean: kinematic constraints. *Tectonophysics* 468, 98–112. <http://dx.doi.org/10.1016/j.tecto.2008.12.016>.
- Aslanian, D., Moulin, M., 2013. Palaeogeographic consequences of conservational models in the South Atlantic Ocean. In: Mohriak, W.U., Danforth, A., Post, P.J., Brown, D.E., Tari, G.C., Nemčok, M., Sinha, S.T. (Eds.), *Conjugate Divergent Margins*. Geol. Soc. (Lond.) Spec. Publ. 369. <http://dx.doi.org/10.1144/SP369.5>.
- Beaumont, C., Ings, S.J., 2012. Effect of depleted continental lithosphere counterflow and inherited crustal weakness on rifting of the continental lithosphere: general results. *J. Geophys. Res.* 117, B08407. <http://dx.doi.org/10.1029/2012JB009203>.
- Begg, G.C., Griffin, W.L., Natapov, L.M., O'Reilly, S.Y., Grand, S., O'Neill, C.J., Poudjom Djomani, Y., Deen, T., Hronske, J., Bowden, P., 2009. The lithospheric architecture of Africa: seismic tomography, mantle petrology, and tectonic evolution. *Geosphere* 5, 23–50. <http://dx.doi.org/10.1130/Ges00179.1>.
- Bronner, A., Sauter, D., Manatschal, G., Péron-Pinvidic, G., Munschy, M., 2011. Magmatic breakup as an explanation for magnetic anomalies at magma-poor rifted margins. *Nat. Geosci.* 4, 549–553. <http://dx.doi.org/10.1038/NGEO1201>.
- Buck, W.R., 1991. Modes of continental lithospheric extension. *J. Geophys. Res.* 96, 20161–20178.
- Chalmers, J.A., Pulvertaft, T.C.R., Christiansen, F.G., Larsen, H.C., Laursen, K.H., Ottesen, T.G., 1993. The southern West Greenland continental margin: rifting history, basin development and petroleum potential. In: Parker, J.R. (Ed.), *Petroleum Geology of Northwest Europe*. In: Proceedings of the 4th Conference. Geological Society, London, pp. 915–931.
- Chenin, P., Beaumont, C., 2013. Influence of offset weak zones on the development of rift basins: activation and abandonment during continental extension and breakup. *J. Geophys. Res.* 118, 1698–1720. <http://dx.doi.org/10.1002/jgrb.50138>.
- Chian, D., Louden, K.E., Reid, I., 1995. Crustal structure of the Labrador Sea conjugate margin and implications for the formation of nonvolcanic continental margins. *J. Geophys. Res.* 100, 24239–24253.
- Contrucci, I., Matias, L., Moulin, M., Gelli, L., Klingelhoefer, F., Nouze, H., Aslanian, D., Olivet, J.-L., Rehault, J.-P., Sibuet, J.-C., 2004. Deep structure of the West African continental margin (Congo, Zaire, Angola), between 5°S and 8°S, from reflection/refraction seismics and gravity data. *Geophys. J. Int.* 158, 529–553.
- Cloetingh, S., Buoy, E., Matenco, L., Beekman, F., Roure, F., Ziegler, P.A., 2013. The Moho in extensional tectonic settings: insights from thermo-mechanical models. *Tectonophysics* 609, 558–604.
- Dean, S.M., Minshull, T.A., Whitmarsh, R.B., Louden, K.E., 2000. Deep structure of the ocean-continent transition in the southern Iberia abyssal plain from seismic refraction profiles; the IAM-9 transect at 40 degrees 20'N. *J. Geophys. Res.* 105, 5859–5885.
- Eilon, Z., Abers, G.A., Jin, G., Gaherty, J.B., 2014. Anisotropy beneath a highly extended continental rift. *Geochim. Geophys. Geosyst.* 15, 545–564. <http://dx.doi.org/10.1002/2013GC005092>.
- Fitz, G., Mann, P., 2013a. Evaluating upper versus lower crustal extension through structural reconstructions and subsidence analysis of basins adjacent to the D'Entrecasteaux Islands, eastern Papua New Guinea. *Geochim. Geophys. Geosyst.* 14. <http://dx.doi.org/10.1002/ggge.20123>.

- Fitz, G., Mann, P., 2013b. Tectonic uplift mechanism of the Goodenough and Fer-gusson Island gneiss domes, eastern Papua New Guinea: constraints from seismic reflection and well data. *Geochem. Geophys. Geosyst.* 14. <http://dx.doi.org/10.1002/ggge.20208>.
- Fraser, S.I., Fraser, A.J., Lentini, M.R., Gawthorpe, R.L., 2007. Return to rifts- the next wave; fresh insights into the petroleum geology of global rift basins. *Pet. Geosci.* 13, 99–104. <http://dx.doi.org/10.1144/1354-079307-749>.
- Fullsack, P., 1995. An arbitrary Lagrangian-Eulerian formulation for creeping flows and its application in tectonic models. *Geophys. J. Int.* 120, 1–23.
- Funck, T., Louden, K.E., 1999. Wide-angle seismic transect across the Torngat Orogen, northern Labrador: evidence for a Proterozoic crustal root. *J. Geophys. Res.* 104 (B4), 7463–7480. <http://dx.doi.org/10.1029/1999JB900010>.
- Funck, T., Hopper, J.R., Larsen, H.C., Louden, K.E., Tucholke, B.E., Holbrook, W.S., 2003. Crustal structure of the ocean-continent transition at Flemish Cap; seismic refraction results. *J. Geophys. Res.* 108. <http://dx.doi.org/10.1029/2003JB002434>.
- Gleason, G.C., Tullis, J., 1995. A flow law for dislocation creep of quartz aggregates determined with the molten salt cell. *Tectonophysics* 247, 1–23.
- Hopper, J.R., Funck, T., Tucholke, B.E., 2007. Structure of the Flemish Cap margin, Newfoundland: insights into mantle and crustal processes during continental breakup. In: Karner, G., Manatschal, G., Pinheiro, L. (Eds.), *Imaging, Mapping and Modelling Extensional Processes*. Geol. Soc. (Lond.) Spec. Publ. 282, 47–61. <http://dx.doi.org/10.1144/SP282.3>.
- Huismans, R.S., Beaumont, C., 2002. Asymmetric lithospheric extension: the role of frictional-plastic strain softening inferred from numerical experiments. *Geology* 30, 211–214.
- Huismans, R.S., Beaumont, C., 2003. Symmetric and asymmetric lithospheric extension: relative effects of frictional-plastic and viscous strain softening. *J. Geophys. Res.* 108. <http://dx.doi.org/10.1029/2002jb002026>.
- Huismans, R.S., Beaumont, C., 2007. Roles of lithospheric strain softening and heterogeneity in determining the geometry of rifts and continental margins. In: Karner, G., Manatschal, G., Pinheiro, L. (Eds.), *Imaging, Mapping and Modelling Extensional Processes*. Geol. Soc. (Lond.) Spec. Publ. 282, 111–138.
- Huismans, R.S., Beaumont, C., 2008. Complex rifted continental margins explained by dynamical models of depth-dependent lithospheric extension. *Geology* 36, 163–166.
- Huismans, R.S., Beaumont, C., 2011. Depth-dependent extension, two-stage breakup and cratonic underplating at rifted margins. *Nature* 473. <http://dx.doi.org/10.1038/nature09988>.
- Jagoutz, O., Muentener, O., Manatschal, G., Rubatto, D., Péron-Pinvidic, G., Turrin, B.D., Villa, I.M., 2007. The rift-to-drift transition in the North Atlantic: a stuttering start of the MORB machine? *Geology* 35 (12), 1087–1090.
- Japsen, P., Chalmers, J.A., Green, P.F., Bonow, J.M., 2012. Elevated, passive continental margins: not rift shoulders, but expressions of episodic, post-rift burial and exhumation. *Glob. Planet. Change* 90–91, 73–86.
- Jolivet, L., Lecomte, E., Huet, B., Denèle, Y., Lacombe, O., Labrousse, L., Le Pourhiet, L., Mehl, C., 2010. The north Cycladic detachment system. *Earth Planet. Sci. Lett.* 289, 87–104.
- Jones, C.H., Wernicke, B.P., Farmer, G.L., Walker, J.D., Coleman, D.S., McKenna, L.W., Perry, F.V., 1992. Variations across and along a major continental rift: an interdisciplinary study of the Basin and Range province, western USA. *Tectonophysics* 213, 57–96.
- Karato, S.I., Wu, P., 1993. Rheology of the upper mantle: a synthesis. *Science* 260, 771–778.
- Karner, G.D., Driscoll, N.W., Barker, D.H.N., 2003. Syn-rift region subsidence across the West African continental margin; the role of lower plate ductile extension. In: Arthur, T.J., Macgregor, D.S., Cameron, N. (Eds.), *Petroleum Geology of Africa: New Themes and Developing Technologies*. Geol. Soc. (Lond.) Spec. Publ. 207, 105–129.
- Karner, G.D., Driscoll, N.W., McGinnis, J.P., Brumbaugh, W.D., Cameron, N.R., 1997. Tectonic significance of syn-rift sediment packages across the Gabon–Cabinda continental margin. *Mar. Pet. Geol.* 14, 973–1000. [http://dx.doi.org/10.1016/S0264-8172\(97\)00040-8](http://dx.doi.org/10.1016/S0264-8172(97)00040-8).
- Keen, C.E., Potter, P., Srivastava, S.P., 1994. Deep seismic reflection data across the conjugate margins of the Labrador Sea. *Can. J. Earth Sci.* 31, 192–205. <http://dx.doi.org/10.1139/e94-016>.
- Keen, C.E., Dickie, K., Dehler, S.A., 2012. The volcanic margins of the northern Labrador Sea: insights to the rifting process. *Tectonics* 31, TC1011. <http://dx.doi.org/10.1029/2011TC002985>.
- Kumar, N., Danforth, A., Nuttall, P., Helwig, J., Bird, D.E., Venkatraman, S., 2013. From oceanic crust to exhumed mantle: a 40 year (1970–2010) perspective on the nature of crust under the Santos Basin, SE Brazil. In: Mohriak, W.U., Danforth, A., Post, P.J., Brown, D.E., Tari, G.C., Nemcok, M., Sinha, S.T. (Eds.), *Conjugate Divergent Margins*. Geol. Soc. (Lond.) Spec. Publ. 369. <http://dx.doi.org/10.1144/SP369.16>.
- Kusznir, N.J., Karner, G.D., 2007. Continental lithospheric thinning and breakup in response to upwelling divergent mantle flow: application to the Woodlark, Newfoundland and Iberia margins. In: Karner, G.D., Manatschal, G., Pinheiro, L., Imaging, M.L. (Eds.), *Mapping and Modelling Continental Lithosphere Extension and Breakup*. Geol. Soc. (Lond.) Spec. Publ. 282, 389–419.
- Li, L., Clift, P.D., Stephenson, R., Nguyen, H.T., 2014. Non-uniform hyper-extension in advance of seafloor spreading on the Vietnam continental margin and the SW China Sea. *Basin Res.* 26, 106–134. <http://dx.doi.org/10.1111/bre.12045>.
- Lister, G.S., Banga, G., Feenstra, A., 1984. Metamorphic core complexes of Cordilleran type in the Cyclades, Aegean Sea, Greece. *Geology* 12, 221–225.
- Lister, G.S., Etheridge, M.A., Symonds, P.A., 1986. Detachment faulting and the evolution of continental margins. *Geology* 14, 246–250.
- Lister, G.S., Etheridge, M.A., Symonds, P.A., 1991. Detachment models for the formation of passive continental margins. *Tectonics* 10, 1038–1064.
- Little, T.A., Baldwin, S.L., Fitzgerald, P.G., Monteleone, B., 2007. Continental rifting and metamorphic core complex formation ahead of the Woodlark spreading ridge, D'Entrecasteaux Islands, Papua New Guinea. *Tectonics* 26. <http://dx.doi.org/10.1029/2005TC001911>.
- Little, T.A., Hacker, B.R., Gordon, S.M., Baldwin, S.L., Fitzgerald, P.G., Ellis, S., Korchniski, M., 2011. Diapiric exhumation of Earth's youngest (UHP) eclogites in the gneiss domes of the D'Entrecasteaux Islands, Papua New Guinea. *Tectonophysics* 510 (1–2), 39–68. <http://dx.doi.org/10.1016/j.tecto.2011.06.006>.
- Louden, K.E., Chian, D., 1999. The deep structure of non-volcanic rifted continental margins. *Philos. Trans. R. Soc. Lond. A* 357, 767–804.
- Mackwell, S.J., Zimmerman, M., Kohlstedt, D.L., 1998. High-temperature deformation of diabase: implications for tectonics on Venus. *J. Geophys. Res.* 103, 975–984.
- McKenzie, D.P., 1978. Some remarks on the development of sedimentary basins. *Earth Planet. Sci. Lett.* 40, 25–31.
- Meyers, J.B., Rosendahl, B.R., Austin, J.A., 1996. Deep-penetrating MCS images of the South Gabon Basin: implications for rift tectonics and post-breakup salt remobilization. *Basin Res.* 8, 65–84.
- Minshull, T.A., Dean, S.M., White, R.S., Whitmarsh, R.B., 2001. Anomalous melt production after continental break-up in the southern Iberia abyssal plain. *Geol. Soc. (Lond.) Spec. Publ.* 187, 537–550.
- Minshull, T.A., Dean, S.M., Whitmarsh, R.B., 2014. The peridotite ridge province in the southern Iberia Abyssal Plain: seismic constraints revisited. *J. Geophys. Res. Solid Earth* 119, 1580–1598. <http://dx.doi.org/10.1002/2014JB011011>.
- Moulin, M., Aslanian, D., Olivet, J.-L., Contrucci, I., Matias, L., Geli, L., Klingelhoefer, F., Nouze, H., Rehault, J.-P., Unterneh, P., 2005. Geological constraints on the evolution of the Angolan margin based on reflection and refraction seismic data (ZaiAngo project). *Geophys. J. Int.* 162, 793–810. <http://dx.doi.org/10.1111/j.1365-246X.2005.02668.x>.
- Müntener, O., Manatschal, G., 2006. High degrees of melt extraction recorded by spinel harzburgite of the Newfoundland margin: the role of inheritance and consequences for the evolution of the southern North Atlantic. *Earth Planet. Sci. Lett.* 252, 437–452. <http://dx.doi.org/10.1016/j.epsl.2006.10.009>.
- Müntener, O., Manatschal, G., Desmurs, L., Pettke, T., 2010. Plagioclase peridotites in ocean-continent transitions: refertilized mantle domains generated by melt stagnation in the shallow mantle lithosphere. *J. Petrol.* 51, 255–294. <http://dx.doi.org/10.1093/petrology/egp087>.
- Nagel, T.J., Buck, W.R., 2007. Control of rheological stratification on rifting geometry: a symmetric model resolving the upper plate paradox. *Int. J. Earth Sci.* 96, 1047–1057. <http://dx.doi.org/10.1007/s00531-007-0195-x>.
- Pérez-Gussinyé, M., Ranero, C.R., Reston, T.J., Sawyer, D., 2003. Mechanisms of extension at nonvolcanic margins: evidence from the Galicia interior basin, west of Iberia. *J. Geophys. Res.* 108. <http://dx.doi.org/10.1029/2001JB000901>.
- Péron-Pinvidic, G., Manatschal, G., 2009. The final rifting evolution at deep magma poor passive margins from Iberia–Newfoundland: a new point of view. *Int. J. Earth Sci.* 98, 1581–1597. <http://dx.doi.org/10.1007/s00531-008-0337-9>.
- Péron-Pinvidic, G., Manatschal, G., Osmundsen, P.T., 2013. Structural comparison of archetypal Atlantic rifted margins: a review of observations and concepts. *Mar. Pet. Geol.* 43, 21–47.
- Rey, P.F., Teyssier, C., Whitney, D.L., 2009. The role of partial melting and extensional strain rates in the development of metamorphic core complexes. *Tectonophysics* 477, 135–144.
- Rosendahl, B.R., Mohriak, W.U., Odegard, M.E., Turner, J.P., Dickson, W.G., 2005. West African and Brazilian conjugate margins: crustal types, architecture, and plate configurations. In: Post, P., Olsen, N.C., Palms, D.L., Lyons, K.T., Newton, G.B. (Eds.), *25th GCSSEPM Bob F. Perkins Research Conference: Petroleum Systems of Divergent Margin Basins*. Houston, pp. 261–317.
- Royden, L., Keen, C.E., 1980. Rifting processes and thermal evolution of the continental margin of eastern Canada determined from subsidence curves. *Earth Planet. Sci. Lett.* 51, 343–361.
- Sand, K.K., Wright, T.E., Pearson, G., Nielsen, T.F.D., Makovicky, E., Hutchison, M.T., 2009. The lithospheric mantle below southern West Greenland: a geothermobarometric approach to diamond potential and mantle stratigraphy. *Lithos* 112, 1155–1166.
- Savva, D., Meresse, F., Pubellier, M., Chamot-Rooke, N., Lavier, L., Wong Po, K., Franke, D., Steuer, S., Sapin, F., Auxietre, J.L., Lamy, G., 2013. Seismic evidence of hyper-stretched crust and mantle exhumation offshore Vietnam. *Tectonophysics* 608 (26), 72–83. <http://dx.doi.org/10.1016/j.tecto.2013.07.010>.
- Schenker, F.L., Gerya, T., Burg, J.-P., 2012. Bimodal behavior of extended continental lithosphere: modeling insight and application to thermal history of migmatitic core complexes. *Tectonophysics* 579, 88–103.

- Sibuet, J.-C., Tucholke, B.E., 2013. The geodynamic province of transitional lithosphere adjacent to magma-poor continental margins. In: Mohriak, W.U., Danforth, A., Post, P.J., Brown, D.E., Tari, G.C., Nemcok, M., Sinha, S.T. (Eds.), Conjugate Divergent Margins. Geol. Soc. (Lond.) Spec. Publ. 369. <http://dx.doi.org/10.1144/SP369.15>.
- Sutra, E., Manatschal, G., Mohn, G., Unternehr, P., 2013. Quantification and restoration of extensional deformation along the Western Iberia and Newfoundland rifted margins. *Geochem. Geophys. Geosyst.* 14, 2575–2597. <http://dx.doi.org/10.1002/ggge.20135>.
- Unternehr, P., Péron-Pinvidic, G., Manatschal, G., Sutra, E., 2010. Hyper-extended crust in the South Atlantic: in search of a model. *Pet. Geosci.* 16, 207–215. <http://dx.doi.org/10.1144/1354-079309-904>.
- Van Avendonk, H.J.A., Lavier, L.L., Shillington, D.J., Manatschal, G., 2009. Extension of continental crust at the eastern Grand Banks, Newfoundland. *Tectonophysics* 468, 131–148. <http://dx.doi.org/10.1016/j.tecto.2008.05.030>.
- Van Avendonk, H.J.A., Holbrook, W.S., Nunes, G.T., Shillington, D.J., Tucholke, B.E., Louden, K.E., Larsen, H.C., Hopper, J.R., 2006. Seismic velocity structure of the rifted margin of the eastern Grand Banks of Newfoundland, Canada. *J. Geophys. Res.* 111, B11404. <http://dx.doi.org/10.1029/2005JB004156>.
- Weinberg, R.F., Regenauer-Lieb, K., Rosenbaum, G., 2007. Mantle detachment faults and the breakup of cold continental lithosphere. *Geology* 35, 1035–1038. <http://dx.doi.org/10.1130/G23918A.1>.
- Wernicke, B., 1981. Low-angle normal faults in the Basin and Range province-nappe tectonics in an extending orogeny. *Nature* 291, 645–648.
- Wernicke, B., 1985. Uniform-sense normal simple shear of continental lithosphere. *Can. J. Earth Sci.* 22, 108–125.
- Wernicke, B., 2009. The detachment era (1977–1982) and its role in revolutionizing continental tectonics. In: Ring, U., Wernicke, B. (Eds.), *Extending a Continent: Architecture, Rheology and Heat Budget*. Geol. Soc. (Lond.) Spec. Publ. 321, 1–8.
- Whitmarsh, R.B., Manatschal, G., Minshull, T.A., 2001. Evolution of magma-poor continental margins from rifting to seafloor spreading. *Nature* 413, 150–154.
- Whitney, D.L., Teyssier, C., Rey, P.F., Buck, W.R., 2013. Continental and oceanic core complexes. *Geol. Soc. Am. Bull.* 125, 273–298. 125th Anniversary review paper.
- Zuber, M.T., Parmentier, E.M., Fletcher, R.C., 1986. Extension of continental lithosphere: a model for two scales of Basin and Range deformation. *J. Geophys. Res.* 91, 4826–4838.